

Supporting information

Gold Nanoparticle based Supramolecular Assembly Design for Dye-sensitized H₂-Evolving Photocathodes

Noémie Lalaoui^{#,a,b}, Mohamed Abdellah^{#,a,c}, Kelly L. Materna^a, Bo Xu^a, Haining Tian^a, Anders Thapper^a, Jacinto Sa^{a,d}, Leif Hammarström^{*,a} and Sascha Ott^{*,a}

^a Department of Chemistry-Ångström Laboratories, Uppsala University, Box 523, SE75120 Uppsala, Sweden.

^b Univ. Grenoble Alpes, UMR CNRS 5250, Département de Chimie Moléculaire, 38000 Grenoble, France.

^c Department of Chemistry, Qena Faculty of Science, South Valley University, 83523 Qena, Egypt

^d Institute of Physical Chemistry, Polish Academy of Sciences, 01-224 Warsaw, Poland.

Figure S1. ¹ H NMR spectrum of Co recorded in CD ₂ Cl ₂	3
Figure S2. ATR-IR spectra of 1 (blue) and Co (red).	4
Figure S3. A) Cyclic voltammograms of Co (1 mM) recorded at different scan rates in DMF/0.1 M TBAPF ₆ (second scan) and B) Variation of the cathodic peak currents with the square root of the scan rate. The addition of adamantane moiety did not modify the electrochemical response ¹	4
Figure S4. ¹ H NMR spectrum of PCA recorded in CDCl ₃	5
Figure S5. ATR-IR spectra of PCA. Consistent with what it reported in literature. ²	5
Figure S6. A) UV-vis spectra of PCA in CH ₂ Cl ₂ at various concentration and B) Calibration plot at 503 and 476 nm.	6
Figure S7. Cyclic voltammograms of bare TiO ₂ and TiO ₂ PCA electrodes in MeCN (0.1 M TBAPF ₆). Measurements were carried out at 100 mV·s ⁻¹	6
Figure S8. Cyclic voltammograms of bare NiO and NiO PCA electrodes in MeCN (0.1 M TBAPF ₆). Measurements were carried out at 100 mV·s ⁻¹	7
Figure S9. Transmission UV-Vis spectrum of NiO PCA (grey) and NiO PCA β-CD-AuNPs Co (red). NiO electrodes were used to set the background.	8

Figure S10. Spectroelectrochemistry measurements of PCA on a thin NiO film (1 layer, 0.3 μm) under applied bias of - 1.8 V vs. $\text{Fc}^{+/0}$ in N_2 degassed acetonitrile/0.1 M TBAP. Upon applying the potential, the absorption spectra changed from grey line to the red line. 8

Figure S11. A) TEM image of the obtained AuNPs and B) their size distribution histogram... 9

Figure S12. XPS analysis of screen printed NiO electrode sintered at 450°C in the survey mode. The C 1s peak was used as a reference for energy calibration. The presence of carbon is probably residual from the preparation of NiO..... 9

Figure S13. XPS analysis of a NiO|PCA electrode in the survey mode. The same features are observed as for the NiO electrode except the intensity of the C 1s peak is largely increased due to the presence of the dye on the electrode surface.10

Figure S14. XPS analysis of a NiO|PCA|AuNPs|Co electrode in the survey mode.10

Figure S15. XPS spectrum of the Au 4f region for the NiO|PCA|AuNPs electrode showing the Au 4f_{7/2} and 4f_{5/2} doublet with binding energies of 83.8 and 87.5 eV respectively. These are typical values for Au⁰.11

Figure S16. Chronoamperograms of NiO|PCA| β -CD-AuNPs and NiO|PCA| β -CD-AuNPs|Co photocathodes at an applied bias of -0.1 V vs. Ag/AgCl.11

Figure S17. fs TA spectra of A) ZrO₂|PCA, B) NiO|PCA, and C) NiO|PCA|AuNPs|Co.12

Figure S19. Time traces of A) PCA attached to ZrO₂ and NiO at the GSB and ESA, B) time traces of NiO|PCA and NiO|PCA|AuNPs|Co catalyst at both GSB and ESA.....13

Table S1. Dye and catalyst loadings for the NiO|PCA|β-CD-AuNPs|Co

			Before PEC measurement	After PEC measurement
	PCA	AuNPs (S)	Catalyst (Co)	Catalyst (Co)
NiO PCA	$20 \pm 2 \text{ nmol cm}^{-2}$	Not detected	-	-
NiO PCA AuNPs		detected	-	-
NiO PCA AuNPs Co		detected	$0.5 \pm 0.3 \text{ nmol cm}^{-2}$	$0.4 \pm 0.3 \text{ nmol cm}^{-2}$

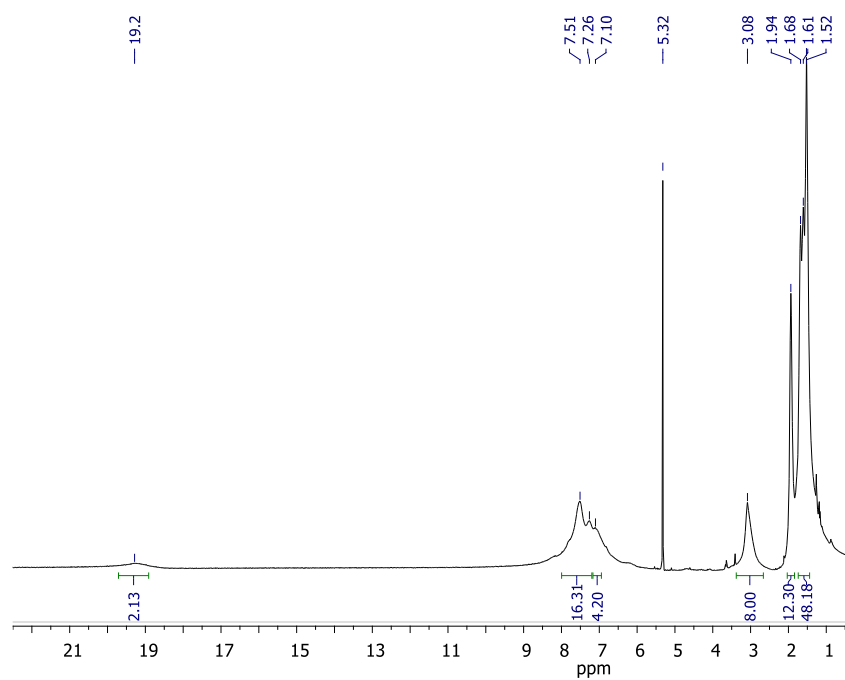


Figure S1. ¹H NMR spectrum of Co recorded in CD₂Cl₂.

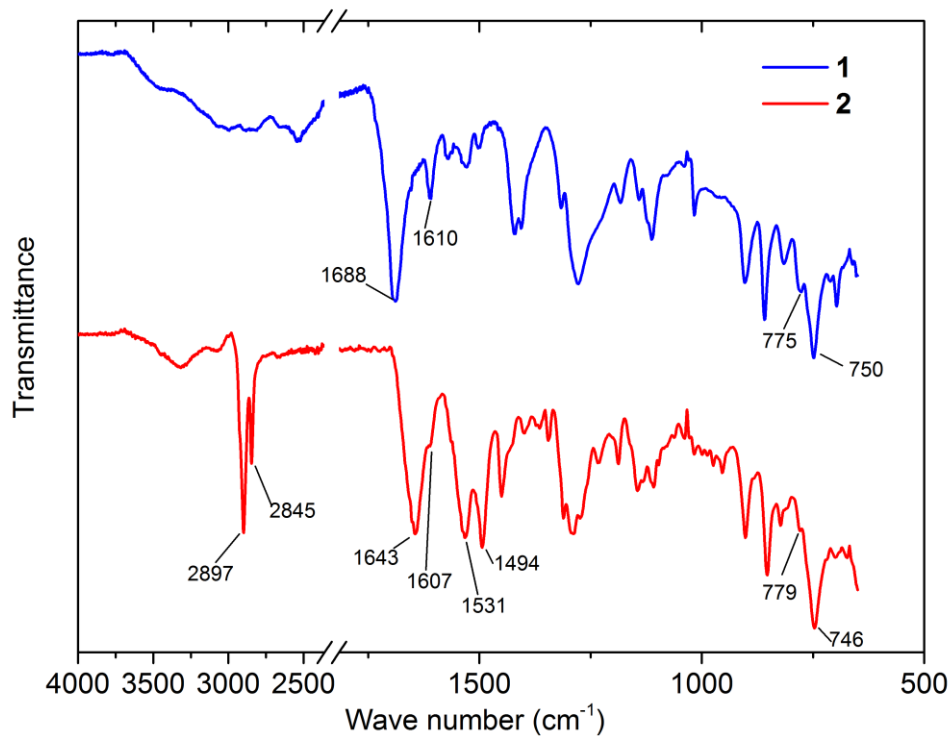


Figure S2. ATR-IR spectra of **1** (blue) and **Co** (red).

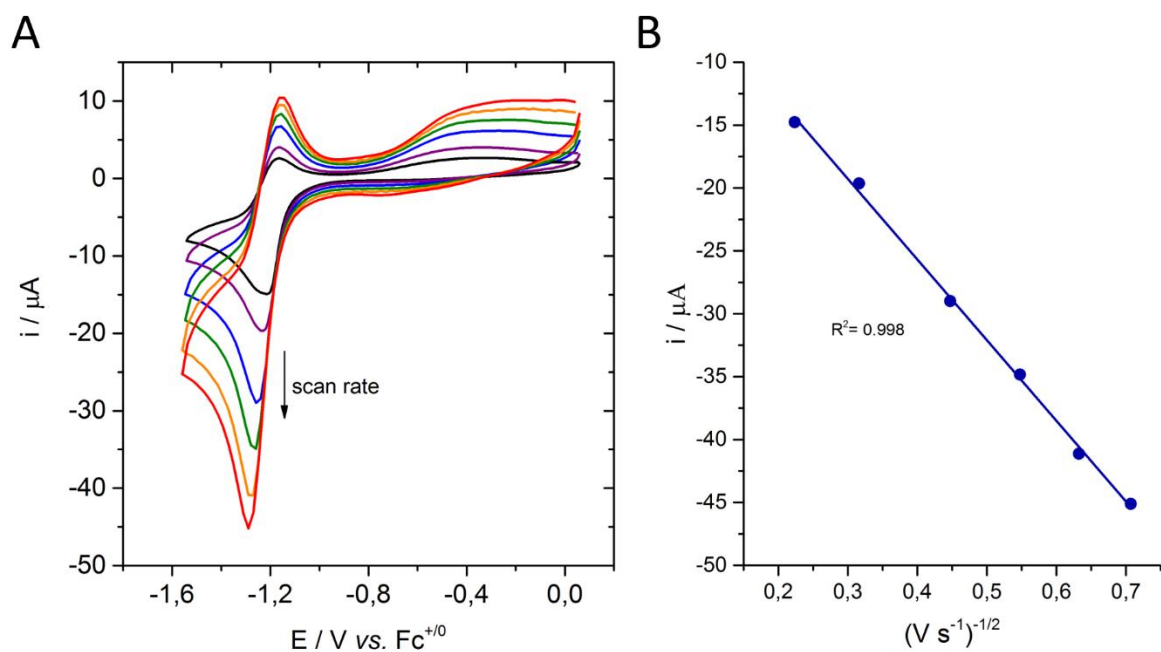


Figure S3. A) Cyclic voltammograms of **Co** (1 mM) recorded at different scan rates in DMF/0.1 M TBAPF₆ (second scan) and B) Variation of the cathodic peak currents with the square root of the scan rate. The addition of adamantane moiety did not modify the electrochemical response¹

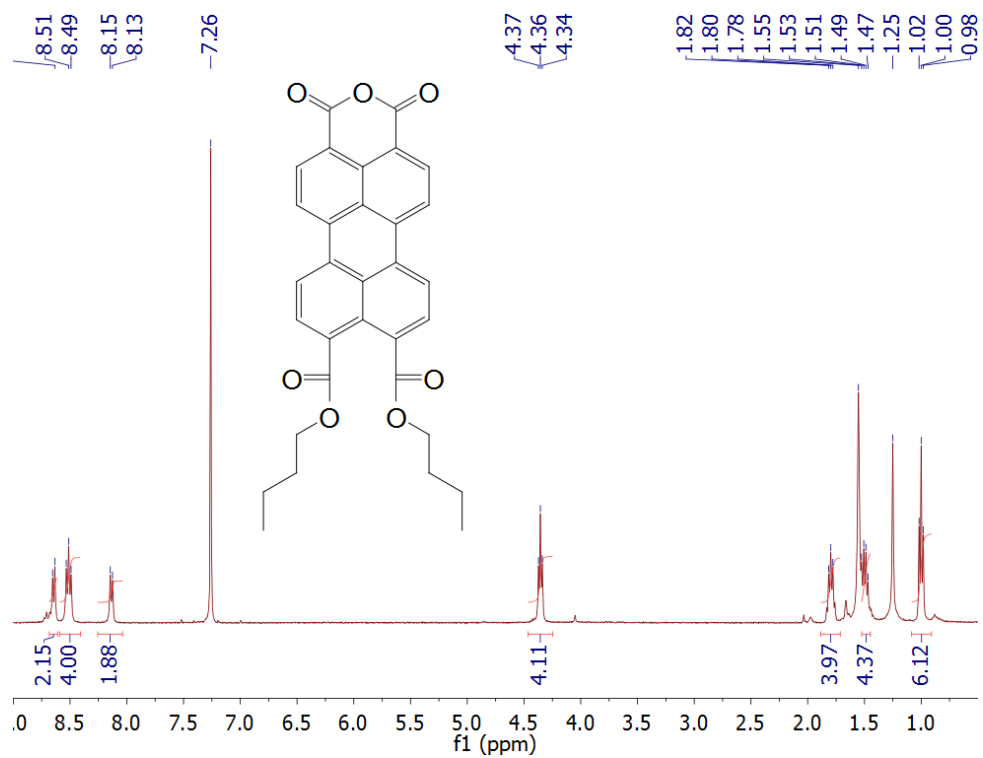


Figure S4. ^1H NMR spectrum of PCA recorded in CDCl_3 .

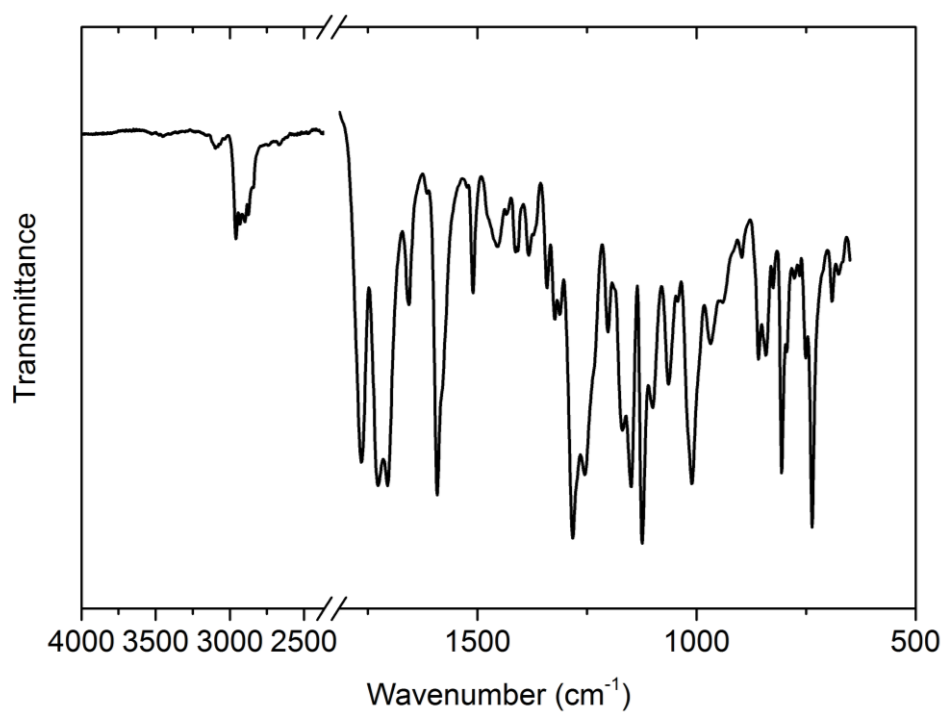


Figure S5. ATR-IR spectra of PCA. Consistent with what it reported in literature.²

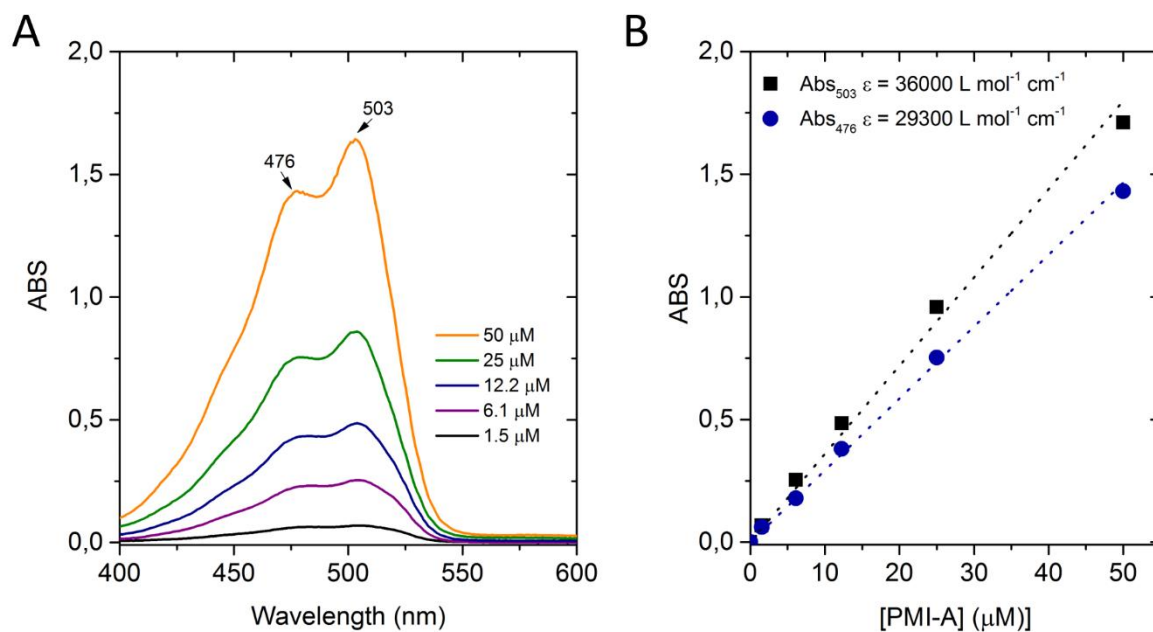


Figure S6. A) UV-vis spectra of PCA in CH₂Cl₂ at various concentration and B) Calibration plot at 503 and 476 nm.

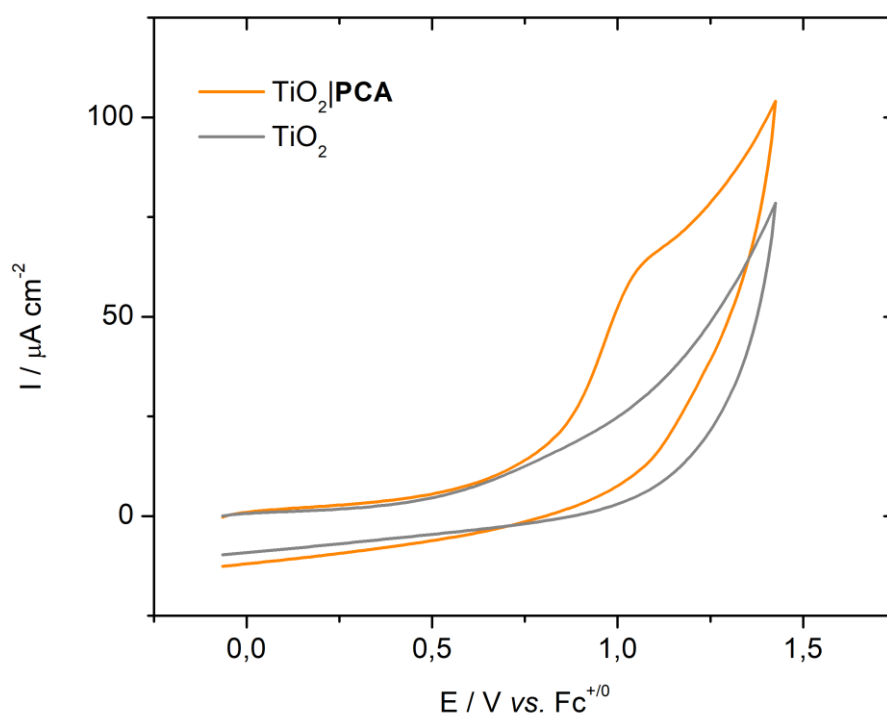


Figure S7. Cyclic voltammograms of bare TiO₂ and TiO₂|PCA electrodes in MeCN (0.1 M TBAPF₆). Measurements were carried out at 100 mV·s⁻¹

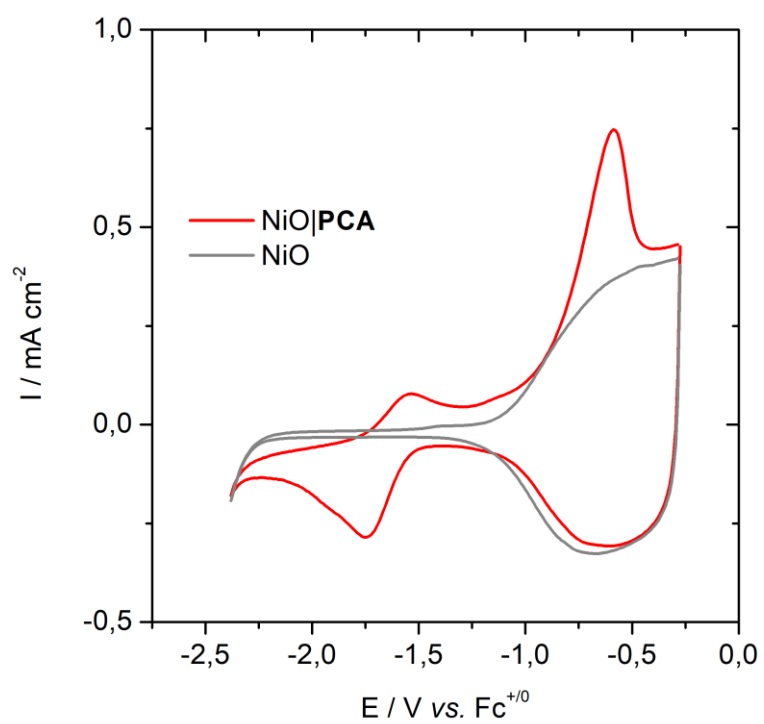


Figure S8. Cyclic voltammograms of bare NiO and NiO|PCA electrodes in MeCN (0.1 M TBAPF₆). Measurements were carried out at 100 mV·s⁻¹

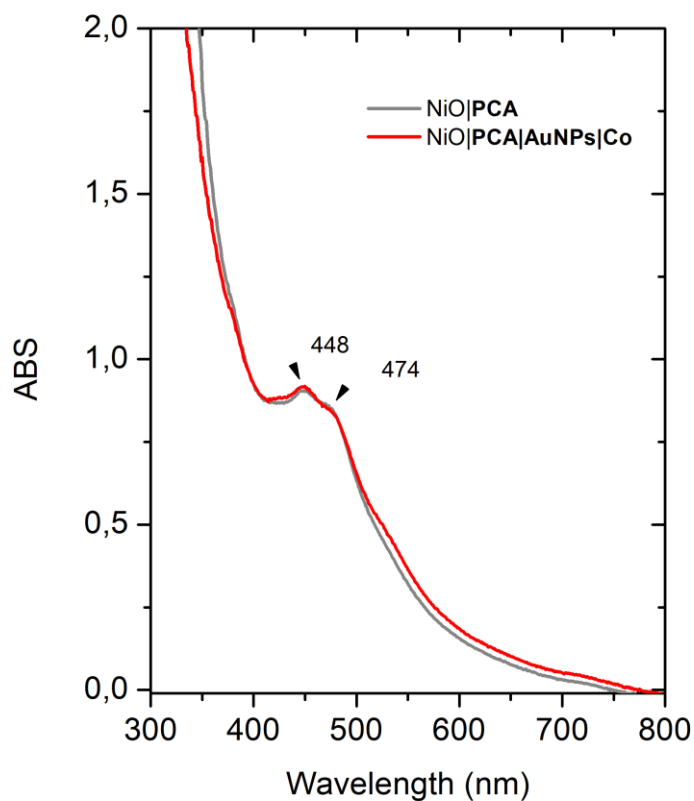


Figure S9. Transmission UV-Vis spectrum of NiO|PCA (grey) and NiO|PCA| β -CD-AuNPs |Co (red). NiO electrodes were used to set the background.

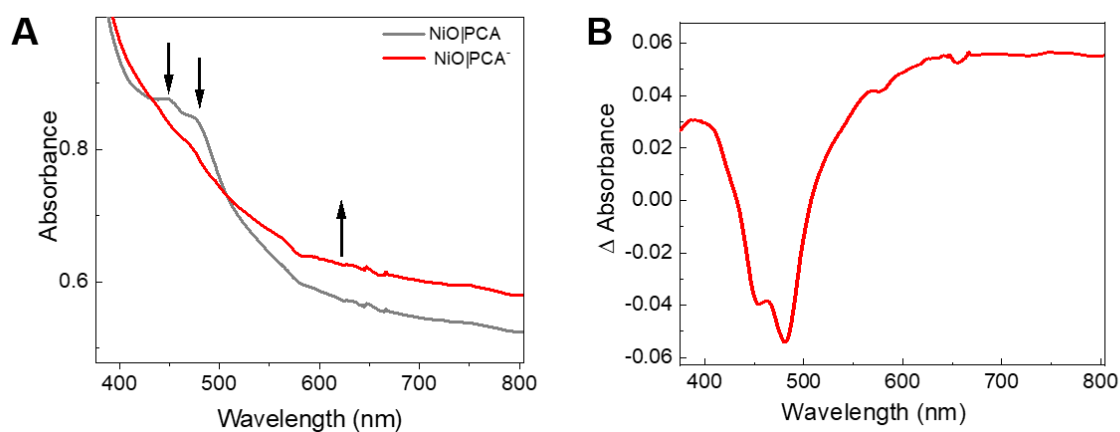


Figure S10. A) Spectroelectrochemistry measurements of PCA on a thin NiO film (1 layer, 0.3 μ m) under applied bias of - 1.8 V vs. $Fc^{+/0}$ in N_2 degassed acetonitrile/0.1 M TBAP. Upon applying the potential, the absorption spectrum changes from the grey line to the red line. B) difference spectrum, highlighting the PCA bleach at 448 and 474 nm and a broad absorption tailing into the red.

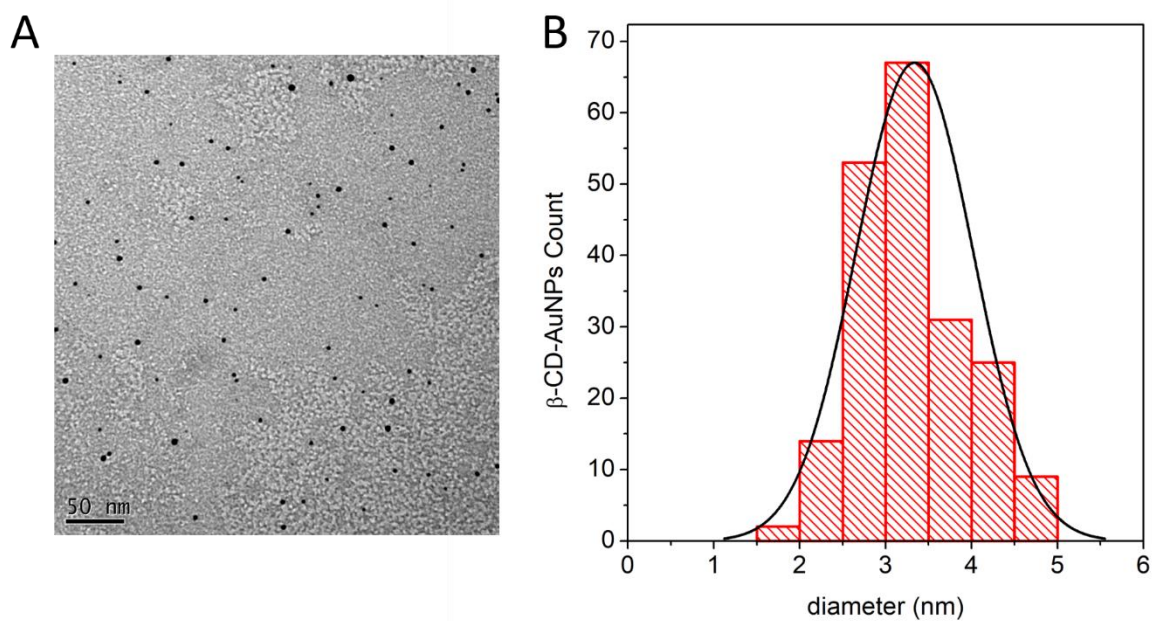


Figure S11. A) TEM image of the obtained AuNPs and B) their size distribution histogram.

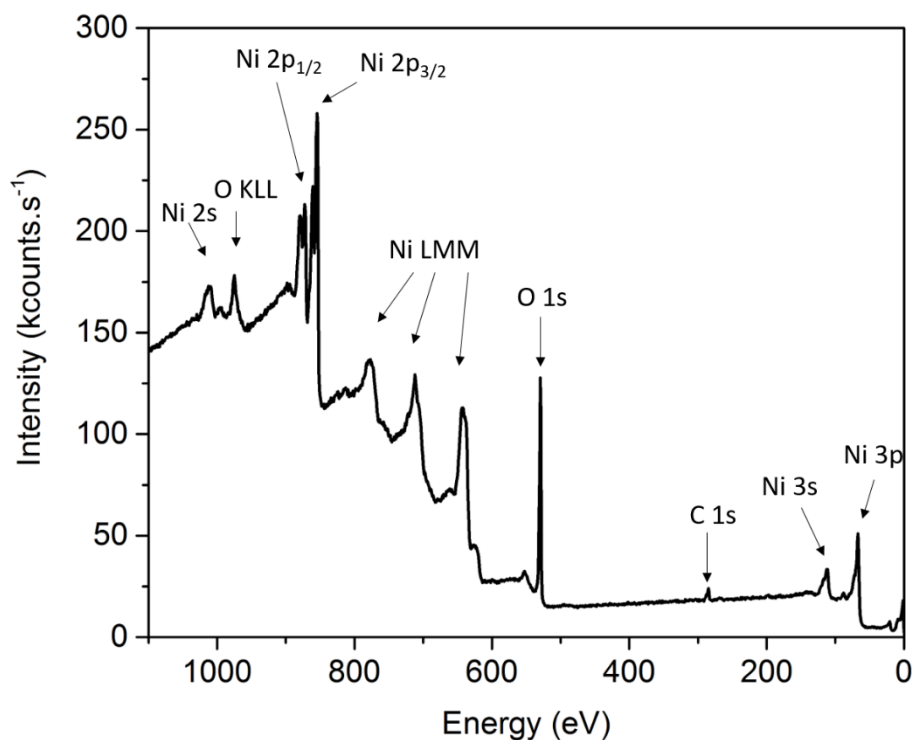


Figure S12. XPS analysis of screen printed NiO electrode sintered at 450°C in the survey mode. The C 1s peak was used as a reference for energy calibration. The presence of carbon is probably residual from the preparation of NiO.

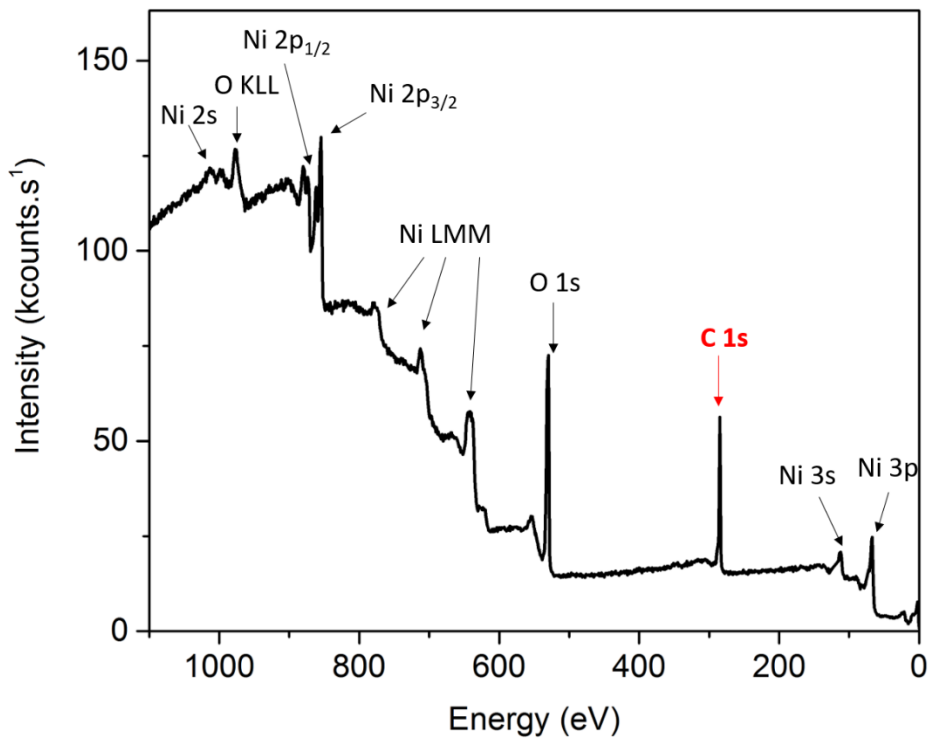


Figure S13. XPS analysis of a NiO|PCA electrode in the survey mode. The same features are observed as for the NiO electrode except the intensity of the C 1s peak is largely increased due to the presence of the dye on the electrode surface.

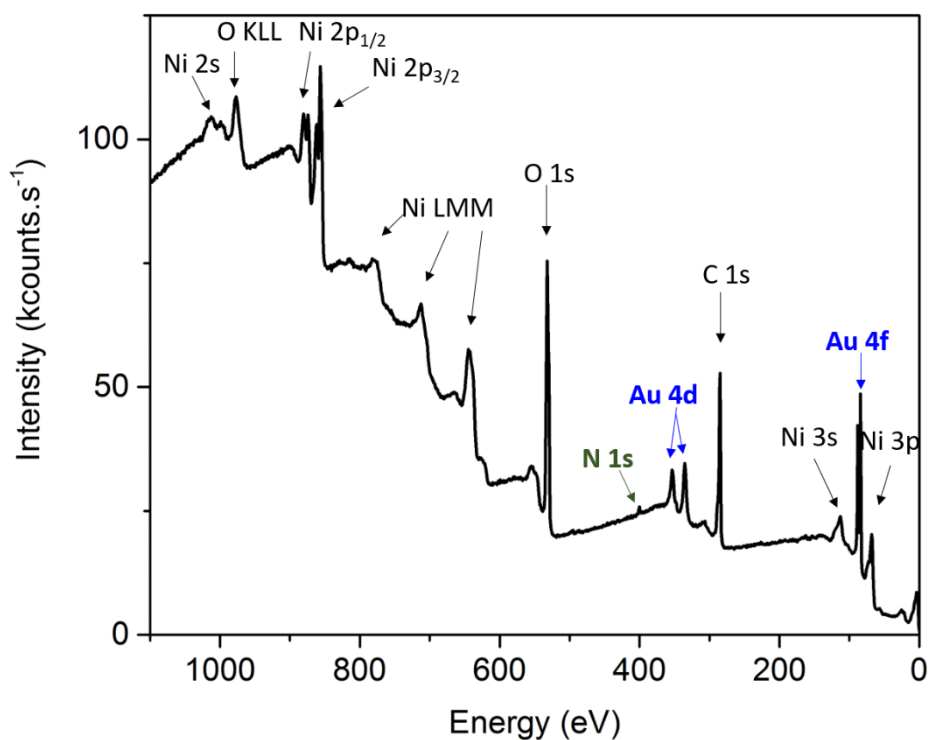


Figure S14. XPS analysis of a NiO|PCA|AuNPs|Co electrode in the survey mode.

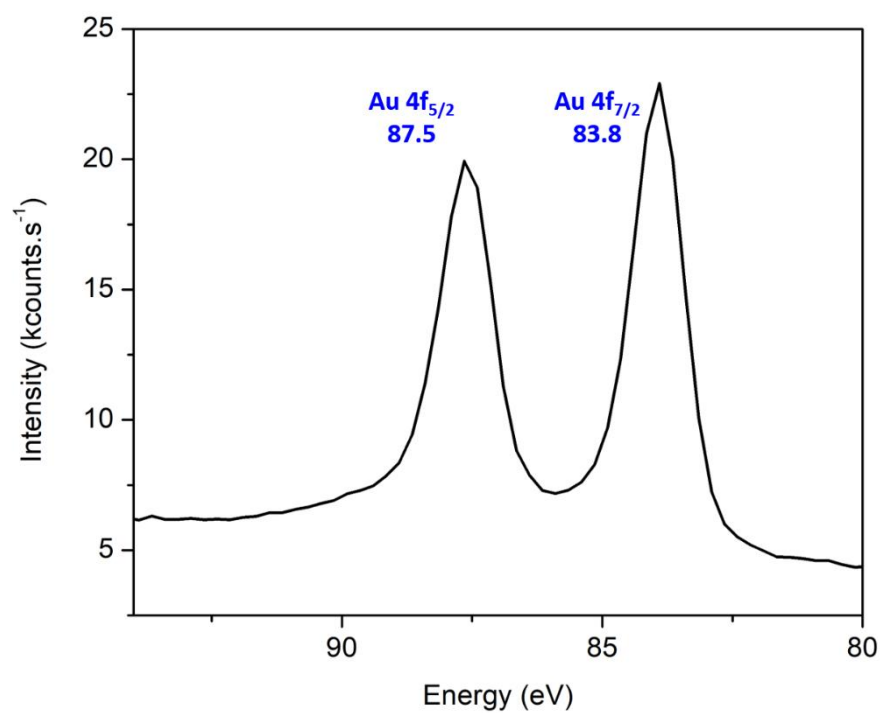


Figure S15. XPS spectrum of the Au 4f region for the NiO|PCA|AuNPs electrode showing the Au 4f_{7/2} and 4f_{5/2} doublet with binding energies of 83.8 and 87.5 eV respectively. These are typical values for Au⁰.

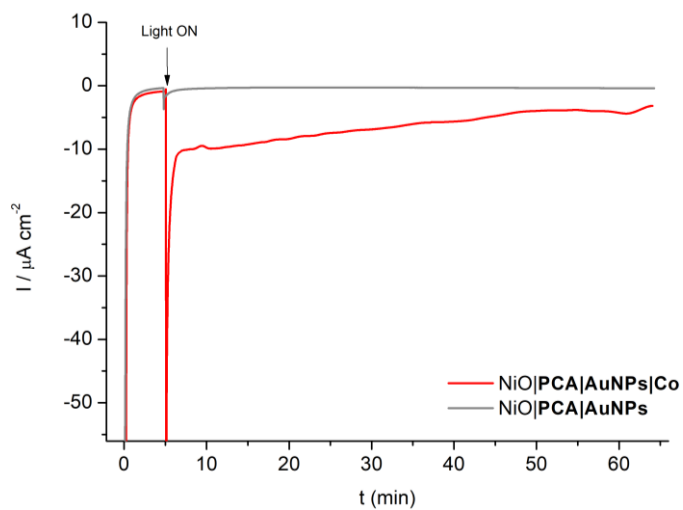


Figure S16. Chronoamperograms of NiO|PCA|β-CD-AuNPs and NiO|PCA|β-CD-AuNPs|Co photocathodes at an applied bias of -0.1 V vs. Ag/AgCl.

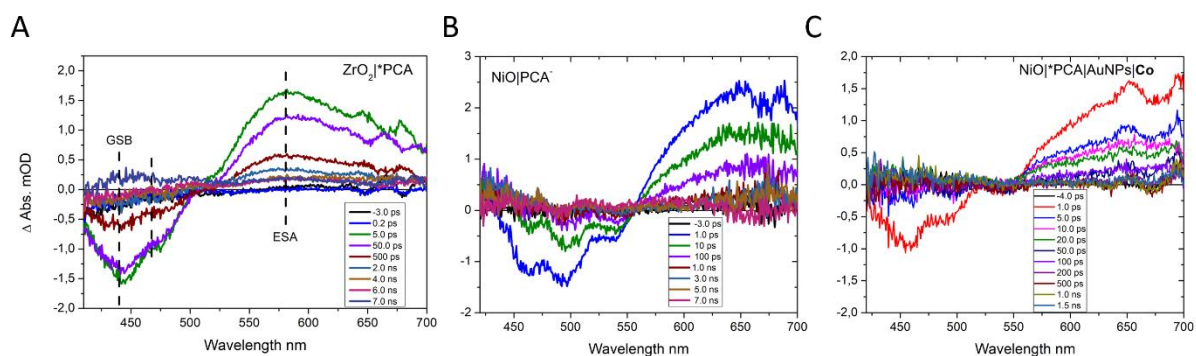


Figure S17. fs TA spectra of A) $\text{ZrO}_2|\text{PCA}$, B) $\text{NiO}|\text{PCA}^-$, and C) $\text{NiO}|\text{PCA}|\text{AuNPs}|\text{Co}$.

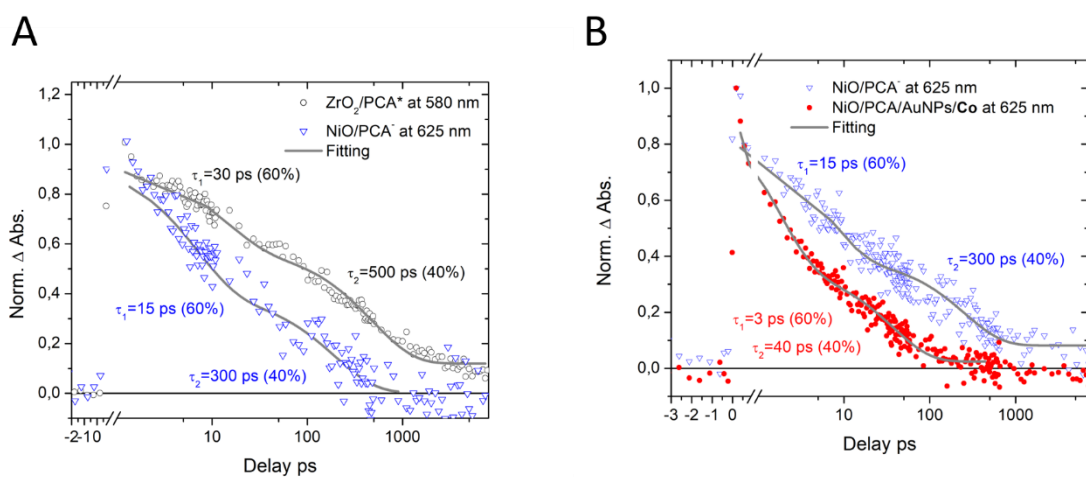


Figure S18. Transient absorption traces of A) $\text{ZrO}_2|\text{PCA}$ at 580 nm (black circles) showing the decay of the excited dye and $\text{NiO}|\text{PCA}$ at 625 nm (blue triangles) showing the decay of the reduced dye ; B) time traces of $\text{NiO}|\text{PCA}^-$ (blue triangles) and $\text{NiO}|\text{PCA}|\text{AuNPs}|\text{Co}$ catalyst (red dots) at 625 nm (reduced dye).

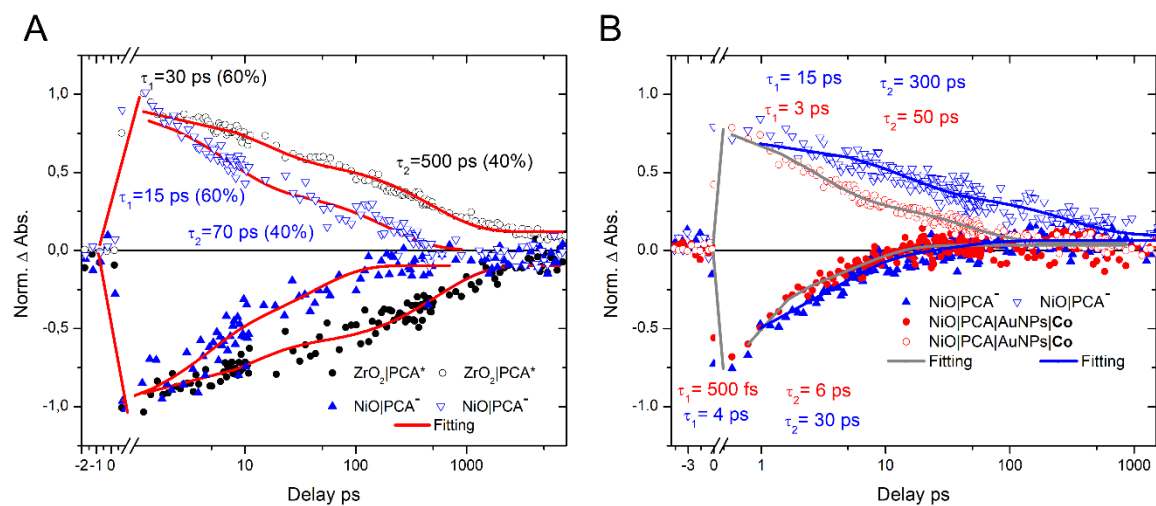


Figure S19. Time traces of A) PCA attached to ZrO₂ and NiO at the GSB (filled) and ESA (empty), B) time traces of NiO|PCA and NiO|PCA|AuNPs|Co catalyst at both GSB (filled) and ESA (empty).

1. Roy, S.; Huang, Z., et al., *J. Am. Chem. Soc.* **2019**, *141* (40), 15942.
2. Webb, J. E. A.; Chen, K., et al., *Physical Chemistry Chemical Physics* **2016**, *18* (3)1712.